Supplementary Information for Publication

Nanoscale Colloids Induce Metabolic Disturbance of Zebrafish at Environmentally Relevant Concentrations

Weilu Kang[a], Xiaokang Li[a], Li Mu[b], Xiangang Hu[a,*]

[a]Key Laboratory of Pollution Processes and Environmental Criteria (Ministry of Education), Tianjin Key Laboratory of Environmental Remediation and Pollution Control, College of Environmental Science and Engineering, Nankai University, Tianjin 300071, China.

[b]Institute of Agro-environmental Protection, Ministry of Agriculture, Tianjin 300191, China

Corresponding authors: Xiangang Hu

Email: huxiangang@nankai.edu.cn

Fax, 0086–022–23507800

Tel, 0086–022–23507800

Sample collection

The Haihe River Basin, which has a drainage area of 3.18×10^5 km^2, is located between 112–120° E and 35–43° N. As the largest water system in the Huabei region of China, the Haihe River plays a vital role in maintaining rapid urban development. The mainstream of Haihe River stems from Sanchakou, flows through Tianjin City and discharges into Bohai Bay. According to the China Environmental Status Bulletin, Tianjin Environmental Quality Statement and Haihe River Water Resources Bulletin in 2016, the Haihe River is heavily polluted, and the main pollutants are heavy metals and organic matter. Industrial, domestic and agricultural effluents have been the main sources of water contamination in recent years. Overall, the Haihe River is a typical contaminated river in China.

For this study, nine sampling sites were selected along the Haihe River. The detailed sampling locations are listed in Table S1. The Haihe River is divided into three sections. Sample locations S1, S2 and S3 are located in the upstream section of the Haihe River, which flows through the uptown and downtown of Tianjin City. The upstream section spans 19 km from Sanchakou to the outer loop and is mainly affected by municipal wastewater pollution. Sample locations S4, S5 and S6 are in the middle reaches of the Haihe River. The middle reaches are located in the countryside between the outer loop and Erdao Gate. This region spans approximately 18 km and serves as a water source for agricultural irrigation, and it is contaminated by agricultural pollution. Sample locations S7, S8 and S9 are situated in the downstream section of the Haihe River and are affected by industrial pollution. S7 and S8 are

located at two dams along the Haihe River that control the water level in the river. S9 is located at the estuary of the Haihe River, which connects the river to the Bohai Sea. Given that the major branches of the Haihe River have a depth range of approximately 6-9 m, water samples were collected at a depth of 2.5-4.5 m below the water surface. At each sampling location, three samples were collected using a 5-L organic glass water sampler on December 8th, 2016 (the temperature was close to the average annual temperature in Tianjin of approximately 12 °C). The samples were stored in polypropylene bottles (500 mL) at 4 °C in the dark and immediately transported to the laboratory for analysis.

Effect of lyophilization on nanoscale colloids

The UV-visible absorption spectra were measured using a UV-vis spectrophotometer (TU-1900, Purkinje General Instrument, China), and the absorption from 200 to 800 nm was recorded. The electrophoretic mobility (EPM) and zeta potential (ζ-potential) were recorded by a Zetasizer Nano instrument (BI-200SM, Brookhaven, USA) equipped with a 30 mW 635 nm laser before and after lyophilization.

Metabolic analysis

A metabolics analysis was performed to further elucidate the molecular mechanisms of nanoscale colloids at 0.45, 4.5, and 45 mg/L. Thirty zebrafish larvae per group were frozen with liquid nitrogen at 120 hpf and then weighed and thoroughly homogenized in 2 mL of precooled 2.5:1:1 v/v/v methanol–chloroform–ultrapure water solution. Afterwards, the homogenate was sonicated in an ice bath at 300 W for 5 min and centrifuged at 11000 g for 10 min at 4 °C. One milliliter of precooled and

mixed 1:1 v/v methanol–chloroform solution was added to the pellets, and the mixture was then sonicated again at 300 W for 5 min. Subsequently, the extraction was centrifuged, and the supernatant was sufficiently mixed with the initial supernatant. The mixture was dried under a gentle nitrogen flow and then lyophilized. A derivatization reaction was performed with 50 μL of O-Methyl amine hydrochloride (20 mg/mL in pyridine) and 80 μL of N-methyl-N-(trimethylsilyl)-trifluoroacetamide at 37 °C for 30 min. After derivatization, the metabolites (1.0 μL) were injected into an Agilent 7683 Series autosampler (Agilent, Atlanta, GA) and analyzed by a gas chromatograph−mass spectrometer (GC-MS, Agilent 7890A-5975C, USA). The detailed GC-MS operation protocol is provided below.

GC-MS operation protocol

The injector temperature was set to 230 °C. Helium was used as the carrier gas, and the gas flow rate through the column was 2 mL/min. The column temperature was initially held at 80 °C for 2 min, increased by 15 °C/ min to 320 °C and then held for 6 min. Both the transfer line and the ion source temperatures were 250 °C. Data acquisition was performed in a full scan mode from m/z 70-600. The acceleration voltage was turned on after a solvent delay of 170 s. The detector voltage was 1700 V. All data were processed in Chroma TOF (Leco Corp., USA). Automatic peak detection and mass spectrum deconvolution were performed using a peak width set to 3.0 s. The values of signal-to-noise (S/N) lower than 10 were rejected.

Table S1. Information on the samples

Sample Nos	Locations (N, E)	Mass Concentrations (mg/L)	TOC (mg/L)	IOC (mg/L)	TOC/IOC (%)	C (%)
S1	(39.166,117.182)	6.21±2.13	0.92±0.15	0.39±0.01	2.33±0.44	22.1±4.5
S2	(39.119,117.216)	7.57±1.13	1.16±0.01	0.54±0.12	2.20±0.49	22.7±2.4
S3	(39.118,117.215)	7.66±0.46	0.88±0.42	0.50±0.21	1.82±0.98	18.4±8.3
S4	(39.083,117.246)	5.11±0.54	1.26±0.12	0.51±0.24	2.82±1.07	34.7±4.8
S5	(39.076,117.291)	4.20±0.79	1.24±0.28	0.57±0.23	2.39±0.86	43.3±8.6
S6	(39.023,117.444)	4.34±0.95	1.21±0.28	0.42±0.03	2.87±0.57	37.9±4.1
S7	(38.987,117.548)	3.62±0.32	1.16±0.11	0.42±0.12	2.84±0.55	43.5±2.9
S8	(39.003,117.651)	3.71±0.27	1.21±0.18	0.46±0.05	1.94±0.59	36.5±6.3
S9	(38.986,117.714)	4.48±0.08	1.33±0.09	0.44±0.07	3.34±1.16	39.5±4.0

TOC, total organic carbon; and IOC, inorganic carbon.

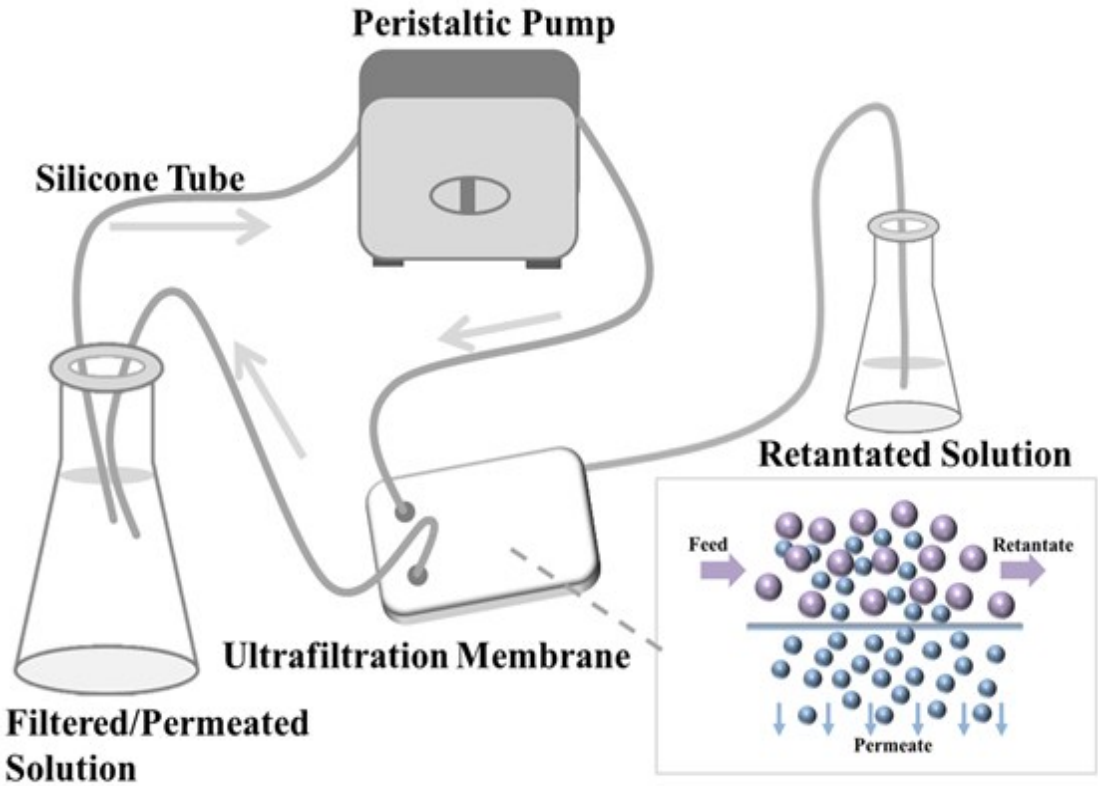

Schema 1. Nanoscale colloids isolated from the Haihe River by a cross-flow filtration (CFF) system.

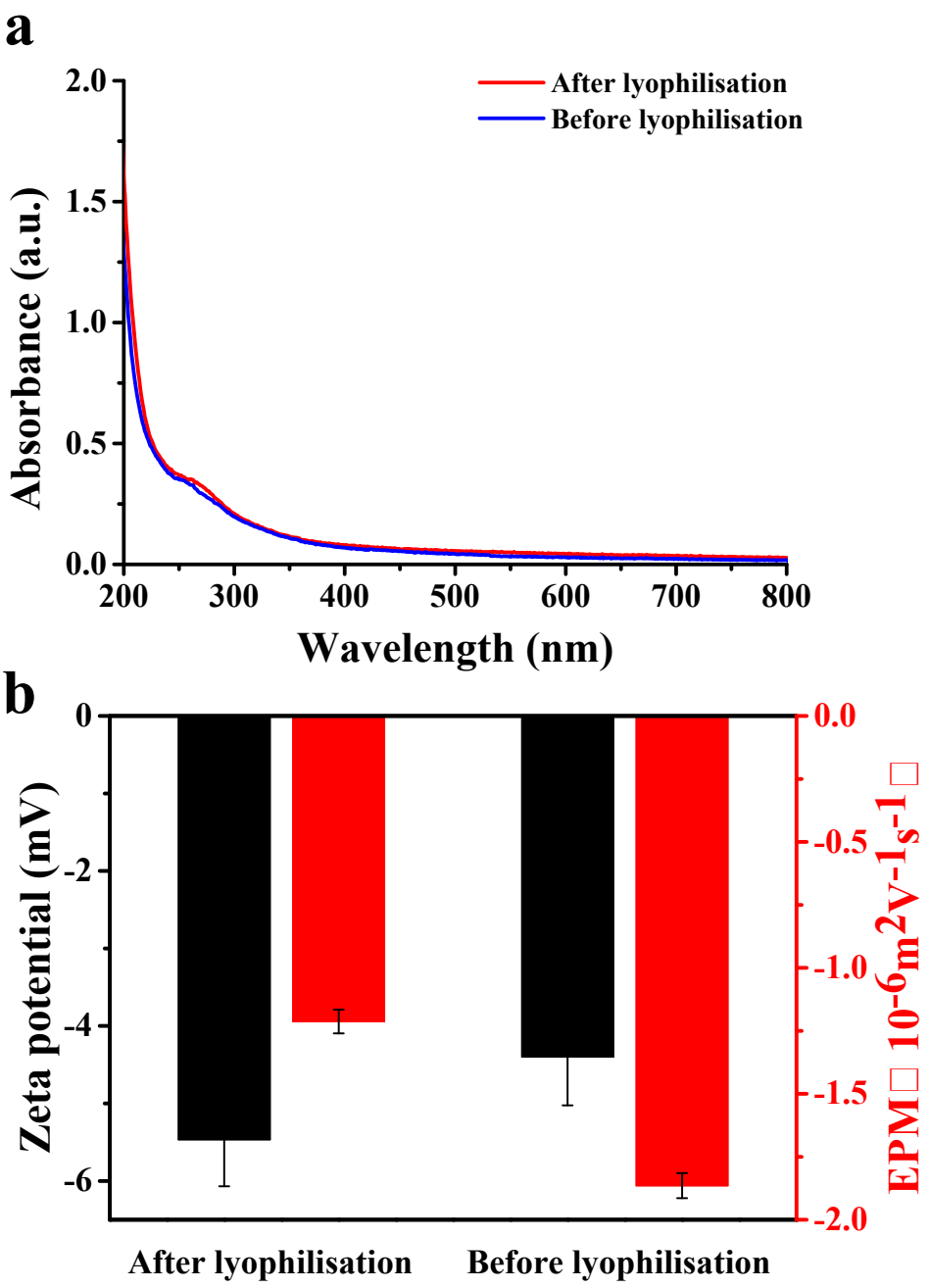

Fig. S1. Effects of freeze-drying on nanoscale colloids before and after lyophilization.

a, UV-vis absorption spectra; b, electrophoretic mobility (EPM) and zeta potential.

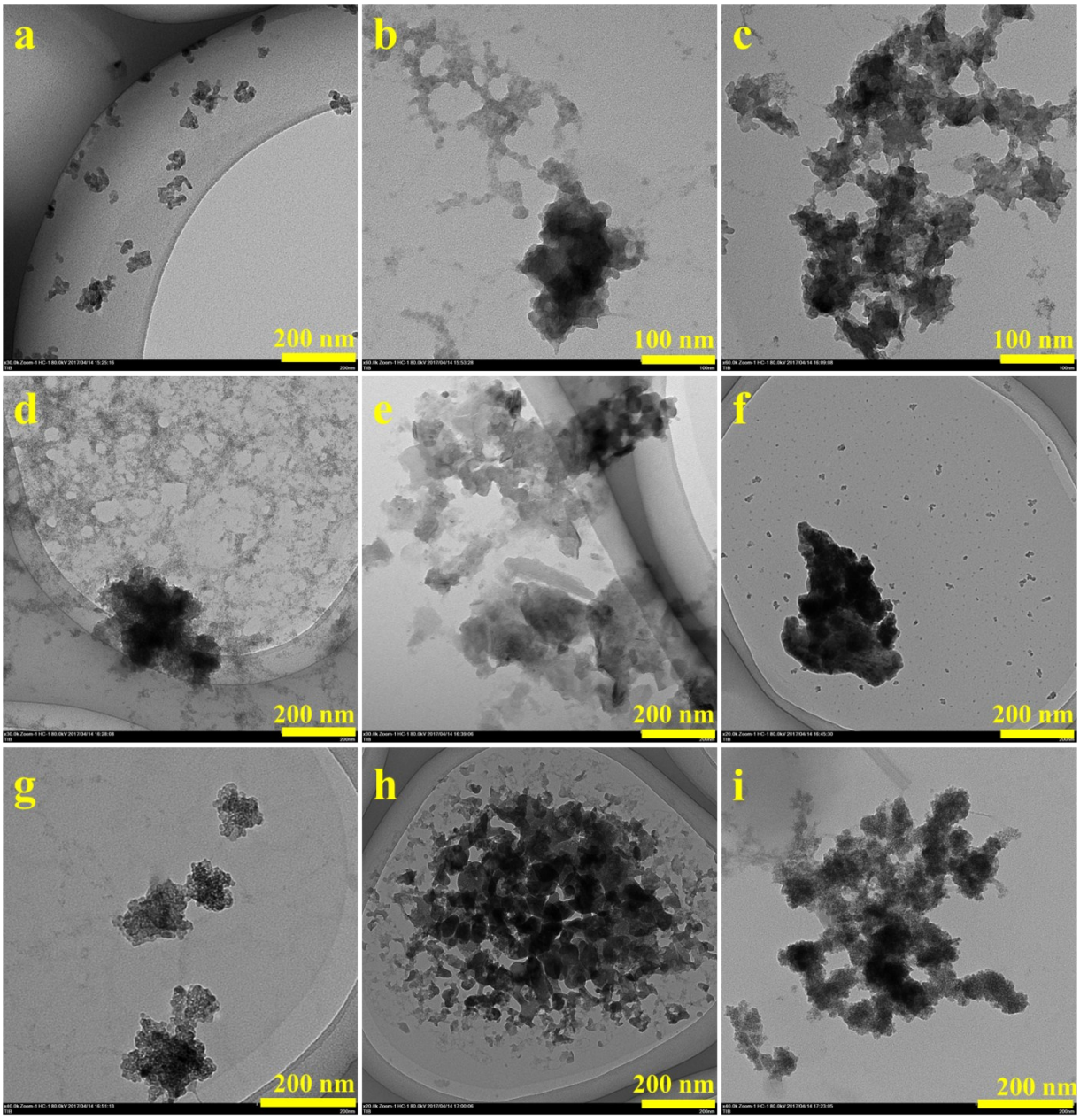

Fig. S2. Transmission electron microscopy (TEM) images of the aggregation of nanoscale colloids. a-f, TEM images of nanoscale colloids extracted from sampling locations S1-S9.

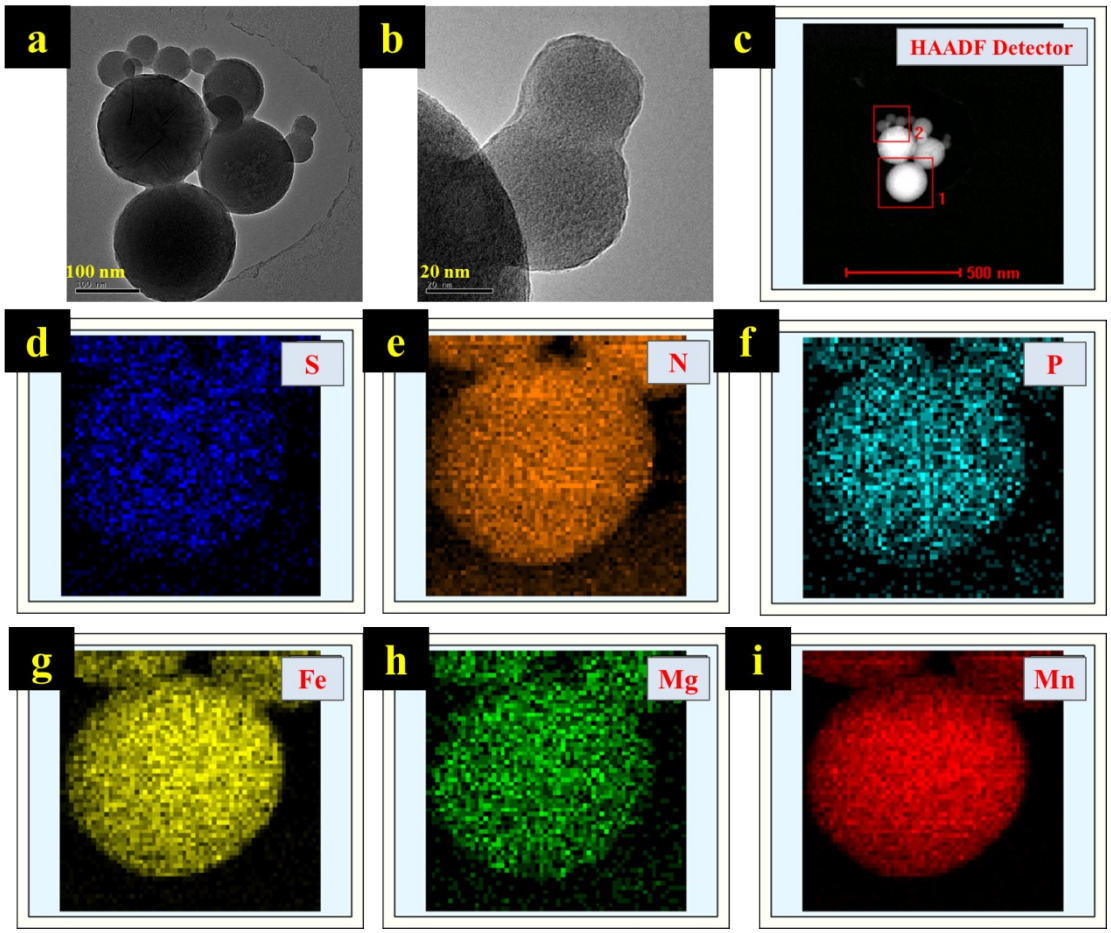

Fig. S3. High-resolution transmission electron microscopy coupled with energy-dispersive X-ray spectroscopy (HRTEM-EDX) mappings of nanoscale colloids extracted from sampling location S4. a and b, TEM images at different scales; c, high-angle annular dark field (HAADF) image; and d-i, elemental mappings of S, N, P, Fe, Mg and Mn.

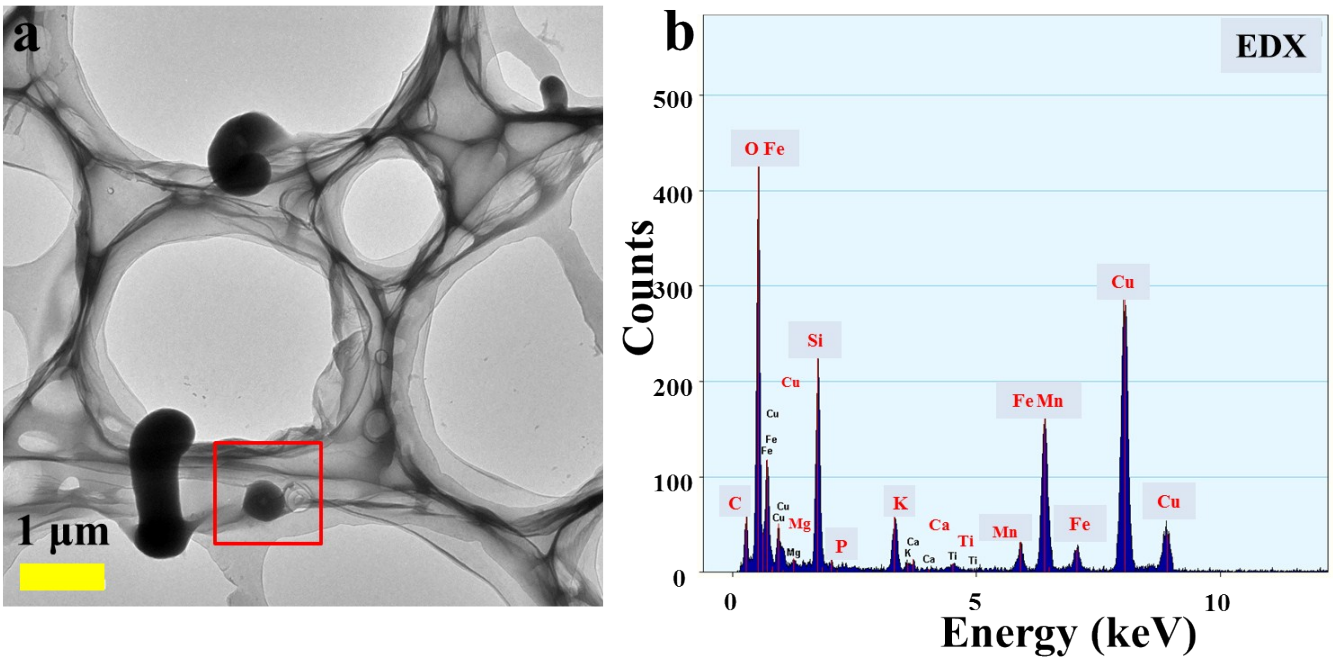

Fig. S4. Energy-dispersive X-ray (EDX) spectra of representative nanoscale colloids.

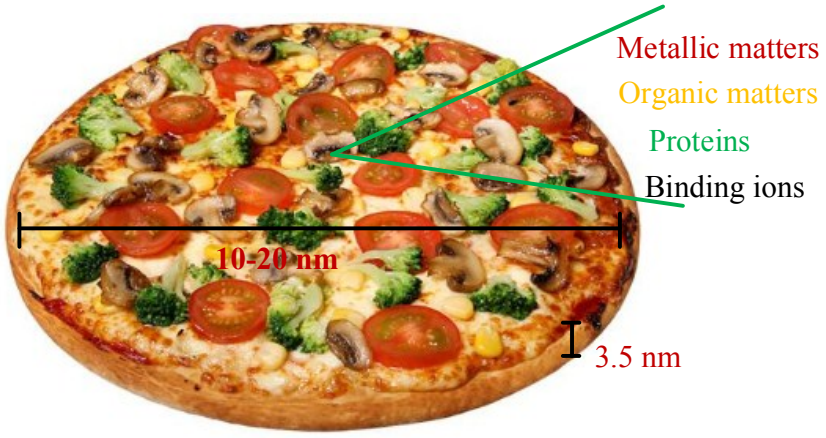

Fig. S5. Diagram of nanoscale colloids with a pizza-like shape and complex composition.

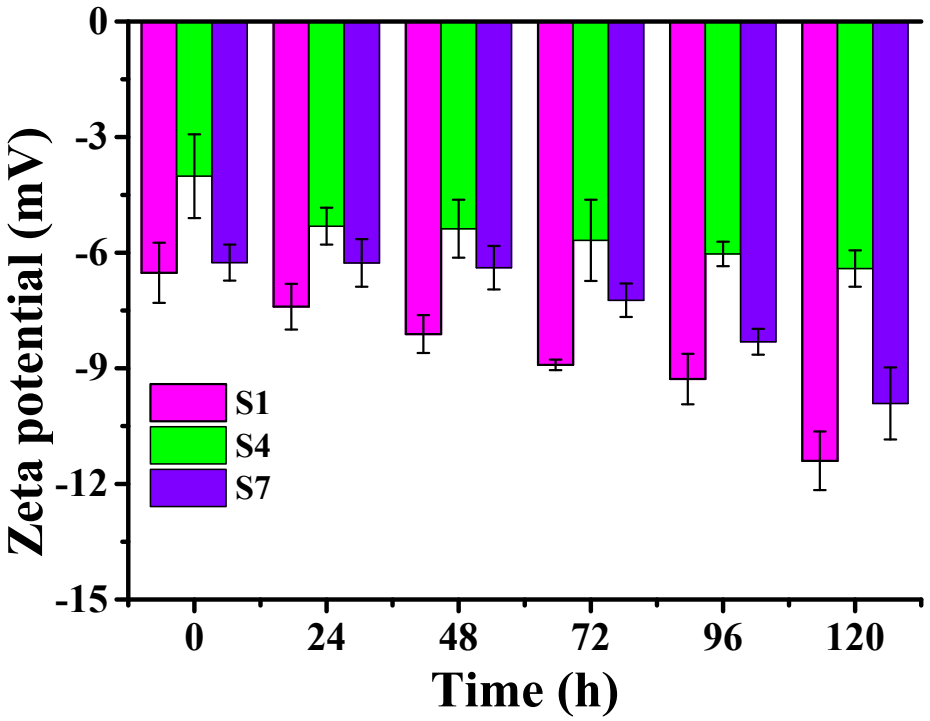

Fig. S6. Zeta potential of nanoscale colloids in deionized water.

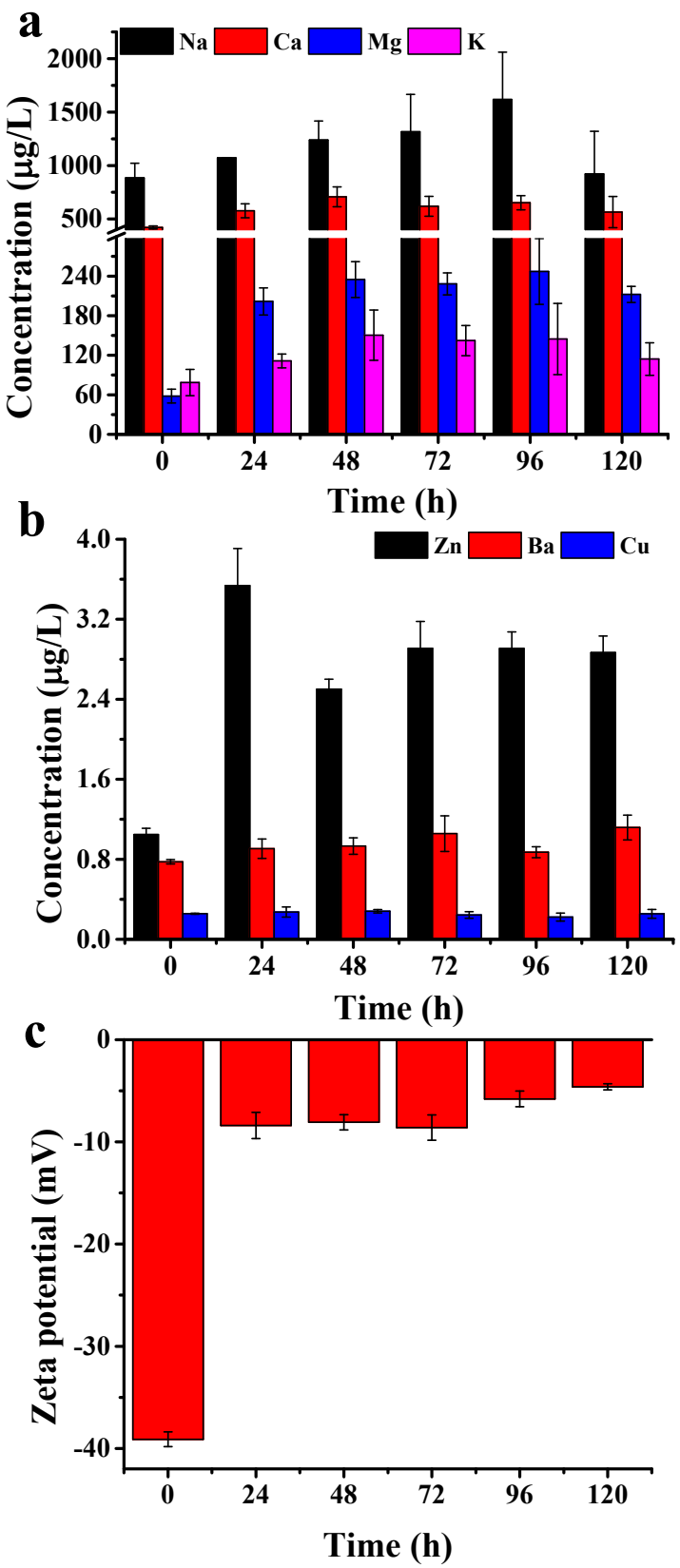

Fig. S7. Stability and release of nanoscale colloids in E3 culture medium. a-b, Metallic ion released from nanoscale colloids. c, Zeta potential.

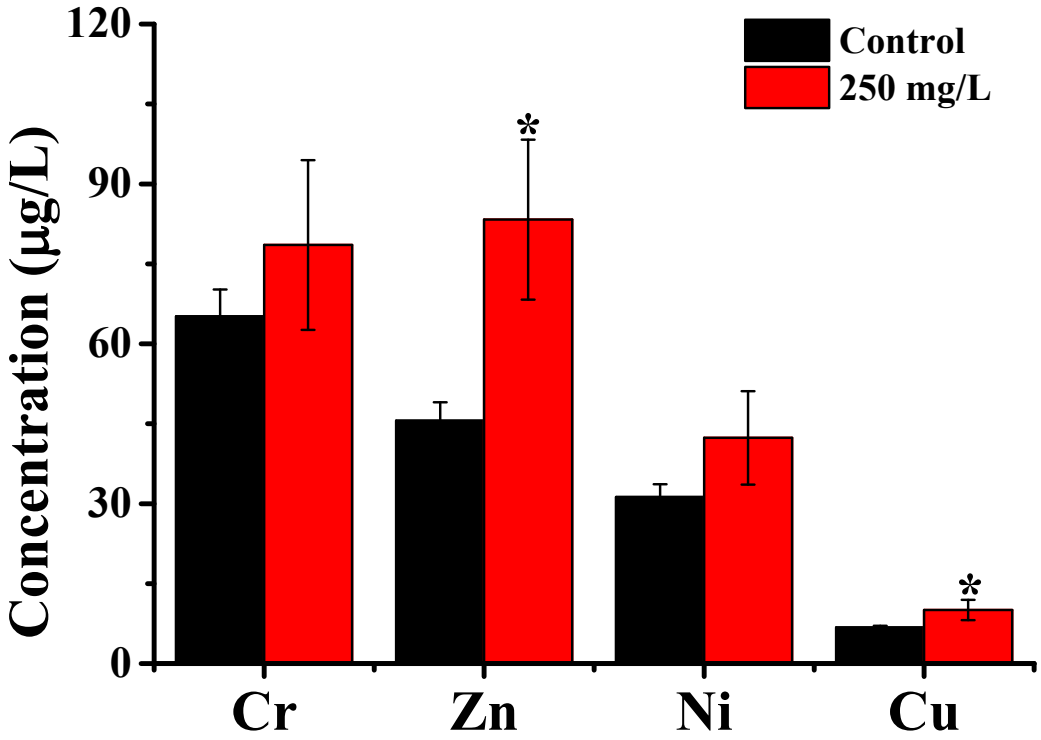

Fig. S8. Chemical analysis on the uptake of nanoscale colloids in zebrafish larvae at 120 hpf. The asterisks (*) represent *p* values < 0.05 between the exposure group and the control group.

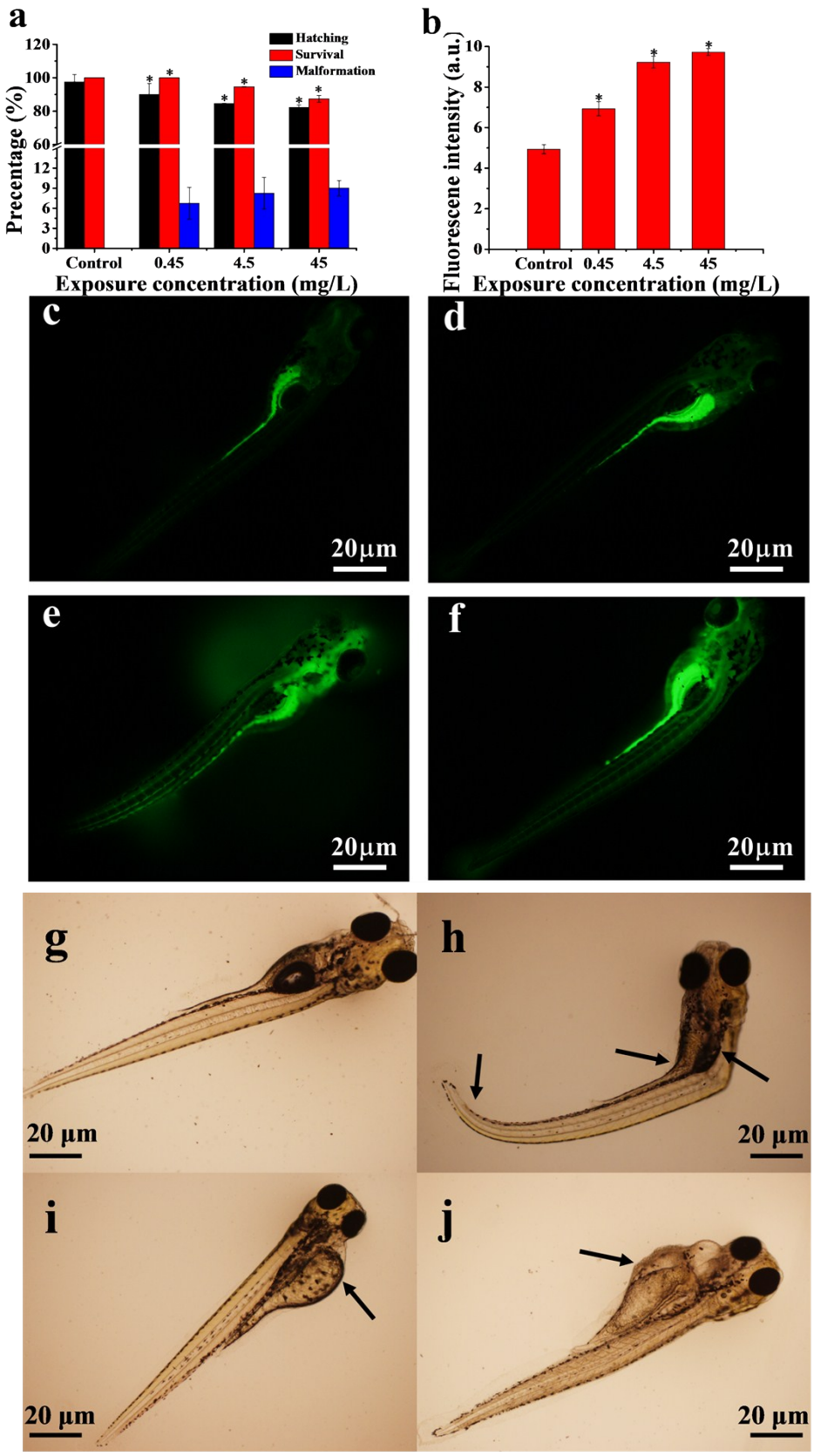

Fig. S9. Effects of nanoscale colloids on zebrafish embryos at 120 hpf. a, Hatching, survival and malformation rates (no malformation was observed in the control); b,

relative fluorescent intensity for reactive oxygen species (ROS) analysis; c-f, fluorescence images of stained larvae for ROS analysis in the control and treatment group (0.45 mg/L, 4.5 mg/L and 45 mg/L); g, no malformation appeared in the control; h, tail flexure, spinal curvature and uninflated swim bladder appeared after treatment with 0.45 mg/L nanoscale colloids; i, yolk sac edema appeared after treatment with 4.5 mg/L nanoscale colloids; and j, pericardial and yolk sac edemas coexisted after treatment with 45 mg/L nanoscale colloids. The above phenotypic malformations are denoted by black arrows. The asterisks (*) represent p values < 0.05 between the treatment groups and the control group.

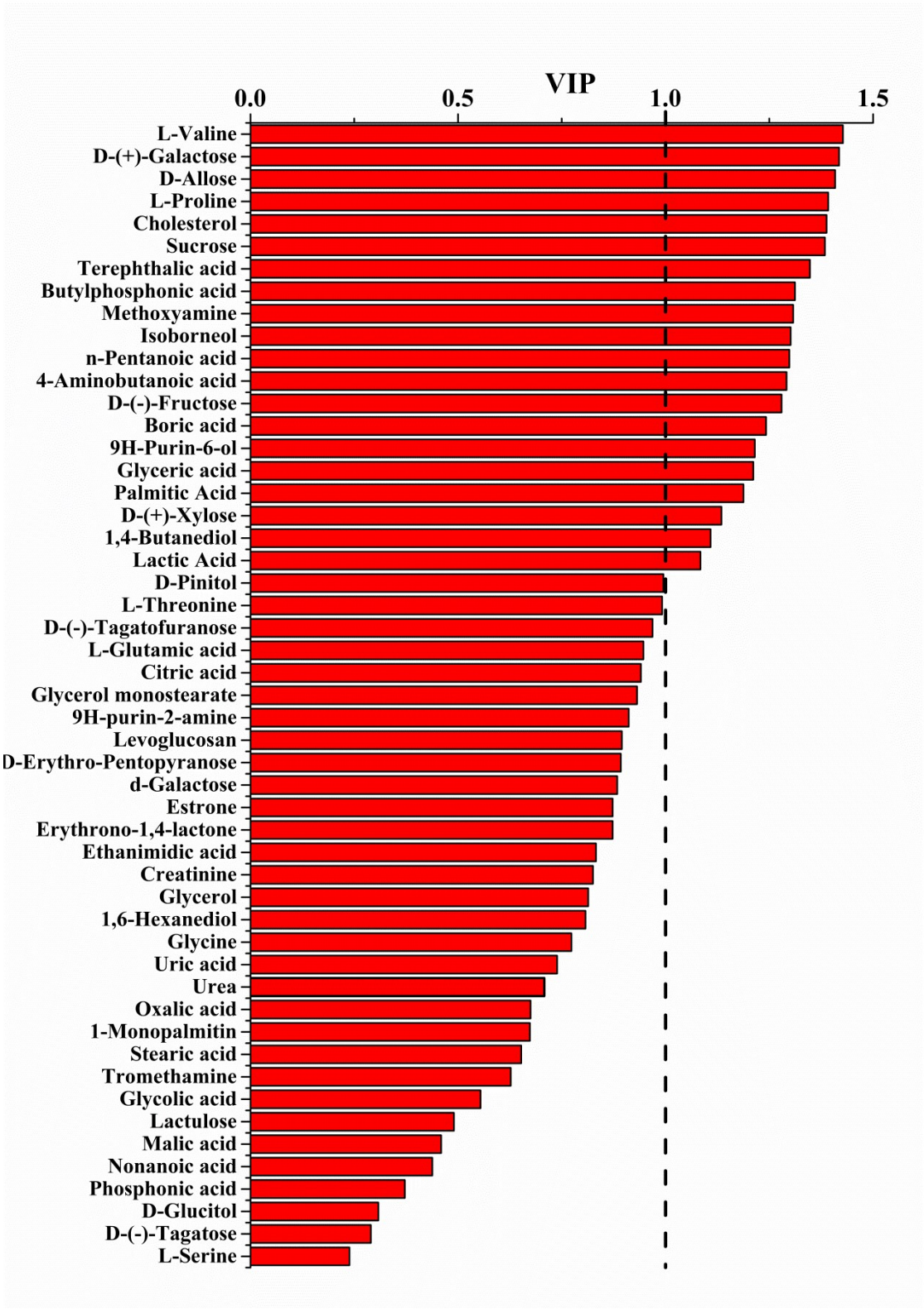

Fig. S10. Variable importance in projection (VIP) from the orthogonal partial least squares discriminant analysis. The abundance of metabolite and the level of reactive oxygen species were set as the X and Y variables, respectively. The black dotted line cuts VIP values off at 1.0.

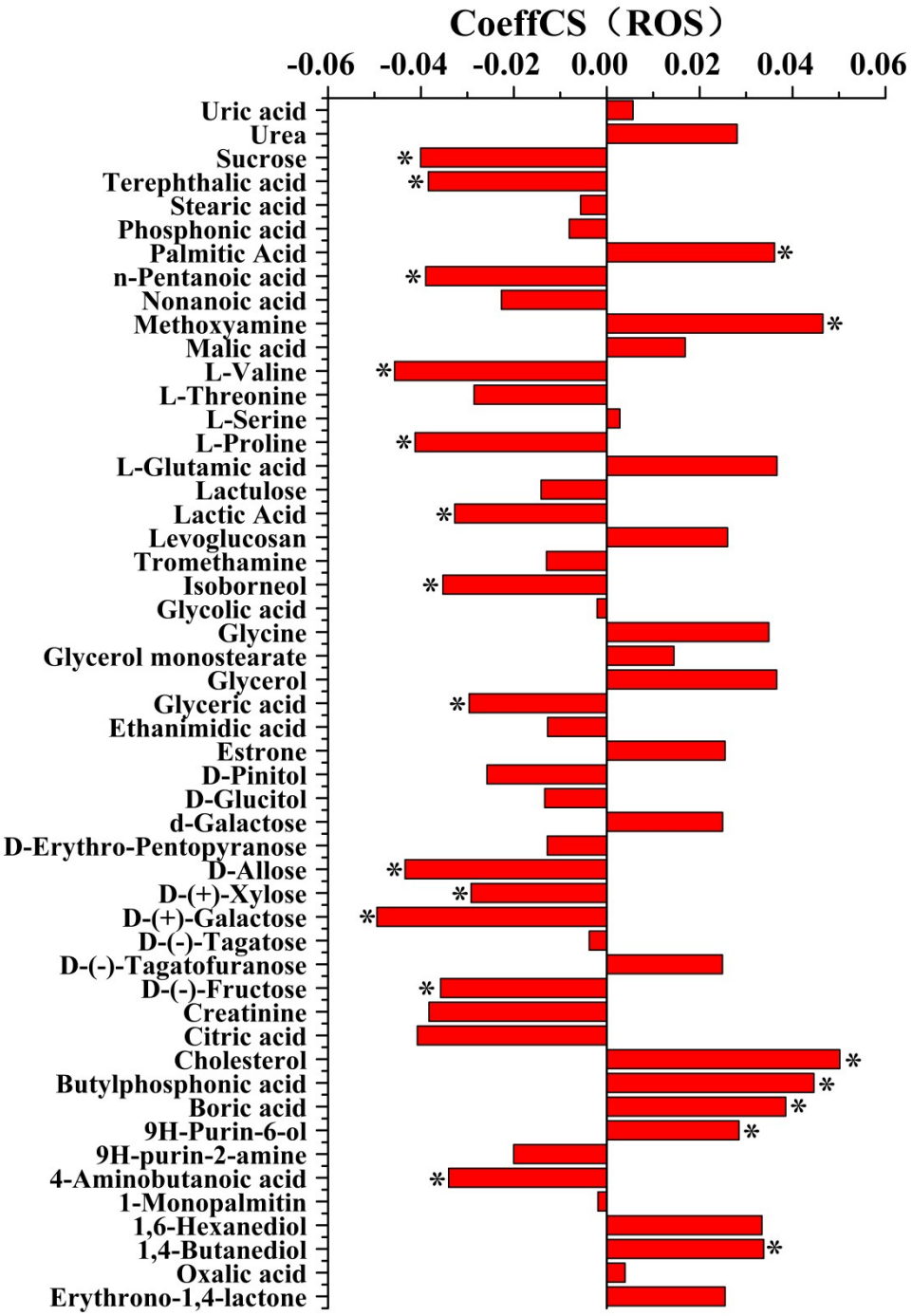

Fig. S11. Centered and scaled coefficient (CoeffCS) values analyzed by OPLS-DA. The abundance of metabolite and the level of reactive oxygen species (ROS) were set as the X and Y variables, respectively. The asterisks (*) indicate the metabolites with variable importance in projection (VIP) > 1.0.